

Environmental Science Processes & Impacts

Accepted Manuscript



This is an *Accepted Manuscript*, which has been through the Royal Society of Chemistry peer review process and has been accepted for publication.

Accepted Manuscripts are published online shortly after acceptance, before technical editing, formatting and proof reading. Using this free service, authors can make their results available to the community, in citable form, before we publish the edited article. We will replace this *Accepted Manuscript* with the edited and formatted *Advance Article* as soon as it is available.

You can find more information about *Accepted Manuscripts* in the [Information for Authors](#).

Please note that technical editing may introduce minor changes to the text and/or graphics, which may alter content. The journal's standard [Terms & Conditions](#) and the [Ethical guidelines](#) still apply. In no event shall the Royal Society of Chemistry be held responsible for any errors or omissions in this *Accepted Manuscript* or any consequences arising from the use of any information it contains.

Combination of DGT and DET can assess redox zonation and mercury methylation in sediments



Environmental impact

In the present study, DGT and DET techniques were used to investigate biogeochemistry and Hg methylation in sediment taken from the Tien River on the Mekong Delta in Vietnam. The robust in-situ techniques revealed that Hg methylation was active during the transition between aerobic and anaerobic sulfate reducing environments. In addition, the depth that showed sulfate reduction was shallower in brackish water sediment than in fresh water sediment, leading to eight times greater methylmercury flux to overlying water in brackish environments. This study shows that co-deployment of various gel-type probes could be extremely helpful in investigating Hg methylation processes coupled with complex biogeochemical reactions and their impact on aquatic environments.

1 **Application of Diffusive Gel-Type Probes for**
2 **Assessing Redox Zonation and Mercury Methylation**
3 **in Mekong Delta Sediment**

4
5 Yongseok Hong¹, Nguyen Phuoc Dan², Eunhee Kim³, Hyo-Jung Choi³, Seunghee Han^{3*}

6 ¹Department of Environmental Engineering, Daegu University, Daegu, Republic of Korea

7 ²Faculty of Environment and Natural Resources, Ho Chi Minh City University of Technology,
8 Ho Chi Minh City, Vietnam

9 ³School of Environmental Science and Engineering, Gwangju Institute of Science and
10 Technology (GIST), Gwangju, Republic of Korea

11
12 * Corresponding author contact: shan@gist.ac.kr

13

14

15

16

17

18

19

20

21

22

23

24 **Abstract**

25 The vertical profiles of PO_4^{3-} , Mn, Fe, S^{2-} , Hg, and CH_3Hg^+ in sediment pore water were
26 investigated using DGT and DET probes in the Tien River, the northern branch of Vietnam's
27 Mekong Delta. Although some of the DGT measurements could be lower than the actual
28 pore water concentrations due to the depletion of the species, the measurements provided
29 information for understanding the redox zonation and Hg methylation. The gradual
30 increases in the measured species concentrations with the sediment depth were observed and
31 the diffusive fluxes of the species to overlying water were expected. Vertical profiles
32 suggested that (1) SO_4^{2-} seemed to be reduced before Fe^{3+} , or the two electron acceptors were
33 reduced simultaneously; (2) the release of PO_4^{3-} was more closely related to S^{2-} than Fe
34 release; and (3) Hg methylation was active in the micro-niche between the aerobic and
35 anaerobic transition zones. Maximum pore water CH_3Hg^+ concentrations were observed at
36 depths just above where the maximum S^{2-} concentrations were detected. Hence, the
37 maximum CH_3Hg^+ concentration was observed near surficial sediments (less than 1 cm from
38 the surface) in brackish water, and the maximum CH_3Hg^+ concentration was observed at a
39 depth of 3 cm in fresh water. The different vertical profiles led to a CH_3Hg^+ diffusive flux
40 eight-times greater in brackish than in fresh water. The present study showed that the *in-situ*
41 application of DGT and DET probes was helpful to understand coupled biogeochemical
42 reactions and mercury methylation by measuring pore water redox species.

43

44 Introduction

45 Since the 1950s, when the Minamata disease in Japan revealed the serious toxicity
46 and environmental persistence of mercury (Hg), understanding of the transport,
47 transformation, fate, and toxicity of Hg in environments and ecosystem has significantly
48 improved.¹⁻³ However, Hg contamination has continuously increased over the last few
49 decades due to the wide usage of Hg in various industrial processes, the release of Hg from
50 coal-fired power plants, biomass burning, and other elements.⁴ Contamination has reached
51 a global scale through Hg transport in the atmosphere, now found in regions as remote and
52 pristine as the Arctic. The human and ecological risks associated with Hg have been
53 recognized as a global problem.² As a result, UNEP (United Nations Environmental
54 Programme) organized an inter-governmental treaty, and more than 150 countries adopted the
55 Minamata Convention in October 2013 to regulate the use and trade of Hg.

56 In aquatic environments, Hg species present in multiple forms, of which
57 monomethylmercury (CH_3Hg^+) is considered the most toxic. The consumption of CH_3Hg^+ -
58 contaminated fish is the most significant exposure route to human and ecological top
59 predators.⁴ The CH_3Hg^+ in fish is primarily produced by microorganisms in anaerobic
60 sediments.^{5,6} The organisms utilize various electron acceptors to create redox zonation
61 (segregation of different terminal electron-accepting processes in separate zones) and release
62 reduced species, such as Mn^{2+} , Fe^{2+} , and S^{2-} .^{7,8} In this way, mercury methylation is tightly
63 coupled with the biogeochemical reactions, a relationship that is critical to understanding
64 how these reactions affect CH_3Hg^+ production.^{9,10}

65 Porewater analysis is necessary to study the biogeochemical reactions; sediment
66 centrifugation and filtration following sediment coring is often used.¹¹ However, the *ex-situ*
67 approach requires lengthy sampling processes including many artifacts, such as physical

68 suspension of colloidal species, exposure to oxygen, and poor resolution. The vertical
69 profiles of the reduced species in sediment pore water is easily disturbed and could be highly
70 variable within a distance of a few millimeters.¹² Accurate characterization of
71 biogeochemical reactions is important in understanding CH_3Hg^+ production and
72 remobilization processes.¹³⁻¹⁷

73 To overcome these limitations, diffusive gradient in thin film (DGT) probes and
74 diffusive equilibrium in thin film (DET) probes are often used.¹⁸ The DGT probe employs a
75 series of layers, including a filter membrane, a diffusive hydrogel, and a resin gel in a plastic
76 unit. The filter side is exposed to the environment, and then dissolved metals diffuse
77 through the hydrogel and are accumulated in the resin gel, which acts as a sink. The DET
78 probe has a configuration similar to DGT, but DET does not have resin gel and only employs
79 a diffusive layer and filter.¹⁹ DET allows the contaminant to disperse to the diffusive layer
80 and achieve equilibrium with the water concentrations. The two techniques have been
81 widely used to detect various trace levels of cationic and anionic species in aquatic
82 environments.^{12,17,18,20-24}

83 In the present study, DGT and DET probes were used to investigate *in-situ*
84 biogeochemical reactions and Hg methylation in the Mekong Delta sediment. The Mekong
85 River spans 4,800 km with a watershed area of 795,000 km². The river discharges 470 km³
86 yr⁻¹ of water, making it the 10th largest river in the world by discharge.²⁵ The Mekong River
87 has water quality problems due to high population density, agricultural activities, and
88 extensive soil erosion in the watershed, which releases nutrients and other contaminants.²⁶
89 Millions of people are dependent on the Mekong Delta and are at risk for Hg exposure
90 through fish consumption.²⁷ Asian countries contribute approximately 50% of the global
91 anthropogenic Hg emissions, of which China accounts for about 60%.²⁸ Regional neighbors
92 such as Vietnam may also be at risk of Hg contamination.

93 In the present study, field sampling was conducted to achieve following two
94 objectives: (1) Application of DGT and DET techniques to measure dissolved PO_4^{3-} , Mn, Fe,
95 S^{2-} , CH_3Hg^+ , and total Hg (THg) in sediment pore water of the Tien River in Vietnam's
96 Mekong Delta; and (2) use of this data to understand how biogeochemical reactions affect
97 CH_3Hg^+ distribution in sediment pore water. The research will be helpful for improving our
98 current understanding on CH_3Hg^+ production in sediments and analyzing the potential risk
99 associated with CH_3Hg^+ in these areas.

100

101 **Materials and methods**

102 **DGT and DET fabrication**

103 DGT and DET probes were prepared according to the procedure described in
104 previous studies.^{18,19,23,29,30} Detailed fabrication processes are presented in the literature,
105 and brief descriptions are provided below and in **Table 1**.

106 Three types of gel solutions were used to prepare resin and diffusive gels. Gel
107 solutions 1, 2, and 3 were abbreviated as GS1, GS2, and GS3; they consisted of 0.3% agarose
108 cross linker+15% acrylamide gel, 1.5% N,N'-methylene bisacrylamide + 28.5% acrylamide,
109 and 1.5% agarose, respectively, in DI water.

110 To make resin gels for THg and CH_3Hg^+ , 1 g of 3-mercaptopropyl functionalized
111 silica gel (3MFSG, Sigma-Aldrich[®]) was mixed with 10 mL of GS1. For polymerization, 60
112 μL ammonium persulfate and 15 μL tetramethylethylenediamine (TEMED) were added to the
113 mixture. The mixture was immediately cast between two glass plates separated by 0.5 mm
114 plastic spacers and allowed to sit at room temperature (22°C) for 2 hours.²⁹

115 To measure S^{2-} , 1 g of finely ground $\text{AgI}_{(s)}$ was dissolved in 10 mL of GS1. After
116 adding 60 μL ammonium persulfate and 15 μL TEMED to the mixture, it was immediately

117 cast between two glass plates separated by 0.5 mm plastic spacers. It is important to keep
118 the AgI_(s) protected from sunlight during the entire AgI resin gel fabrication process, as the
119 AgI could be darkened. However, the gel remains stable when stored in the dark.³⁰

120 To make DGT for PO₄³⁻, ferrihydrite was precipitated, then 24 g of Fe(NO₃)₃·9H₂O
121 was dissolved in 600 mL of deionized water to make 0.1 M Fe³⁺ solution. The pH of the
122 solution was raised to 7.0 by adding 0.1 M or 1 M NaOH to precipitate ferrihydrite. After
123 centrifuging the ferrihydrite slurry at 2500 rpm for 10 minutes, the overlying water was
124 discarded and exchanged with new deionized water. The process was repeated five times to
125 remove any impurities from the ferrihydrite. The water content of the final ferrihydrite
126 precipitate slurry was around 50% (± 5). Then 6 g of the ferrihydrite precipitate was mixed
127 with 10 mL of GS2. After adding 160 μL ammonium persulfate and 16 μL TEMED to the
128 mixture, it was immediately cast between two glass plates separated by 0.5 mm plastic
129 spacers. After casting, the gels were hydrated in deionized water for 24 hours and stored in
130 0.01M NaNO₃ solution at 4°C.²³ This ferrihydrite resin gel has a PO₄³⁻ binding capacity of
131 52 ± 5 μg cm⁻² with an extraction efficiency of 98 ± 12% (n=7), which capacity was large
132 enough to apply for Mekong Delta.

133 After preparing the resin gels, 1.5% agarose diffusive gel with a thickness of 0.75
134 mm was prepared by dissolving 1.5 g of agarose in 100 mL of deionized H₂O on a heating
135 plate. The agarose gel was used to fabricate DGT for THg, CH₃Hg⁺, and PO₄³⁻. Diffusive
136 gel made of GS1 with a thickness of 1.2 mm (0.75 mm multiplied by expansion factor of 1.6)
137 was also prepared and hydrated in DI water for more than 24 hours. The gel was used to
138 fabricate DET for Mn and Fe and DGT for S²⁻.

139 The resin and agarose gels were cut to fit into the disk-type (2-cm diameter) and
140 plate-type DGT (1.5 cm × 15 cm × 0.5 cm) holders, which were purchased from DGT
141 Research Ltd (www.dgtresearch.com). The polysulfone filter (Pall Life Sciences) and

142 PVDF filter (Millipore Corp.) with pore sizes of 0.45 μm were used for disk- and plate-type
143 probes, respectively. For the DET, custom-made plate shape plastic units (2 cm \times 25 cm \times
144 0.5 cm) were used.

145

146 **Site description and DGT/DET deployment**

147 The Mekong Delta has a tropical monsoon climate. Discharge rate and salinity
148 intrusion are significantly dependent on the seasons. During the dry season (November –
149 April), salt water intrusion extends to 70 km inland due to a low discharge rate ($\sim 2,000 \text{ m}^3 \text{ s}^{-1}$).
150 However, during the wet season (May – October), salt water extends only a few km
151 inland due to a high discharge rate ($\sim 40,000 \text{ m}^3 \text{ s}^{-1}$).^{25,27} Considering these patterns of salt
152 water intrusion, the locations were conservatively selected to cover both fresh and estuarine
153 aquatic environments. As shown in **Fig. 1**, five locations were labeled and numbered as L1
154 – L5. These locations were selected downstream of the Tien River, which is among the
155 main rivers that form the delta in Vietnam and discharge into the South China Sea.

156 In each location, DGT probes for THg and CH_3Hg^+ were deployed in the overlying
157 water during a sampling event conducted in September, 2013. In two selected locations,
158 fresh water (L1) and brackish water (L5), DGT probes for THg, CH_3Hg^+ , PO_4^{3-} , and S^{2-} and
159 DET probes for Mn and Fe were deployed. To deploy the probes in overlying water, one
160 end of a 7 mm thick polyethylene line was connected to a navigational buoy, and the other
161 end to a 10 kg concrete block at the bottom of the Tien River. Circular-type DGTs were
162 attached to the line at three different depths (i.e., one close to the air-water interface, one in
163 the middle, and the last at the river's bottom). During the deployment, water temperature,
164 dissolved oxygen, salinity, and conductivity were measured onsite using multi-electrodes
165 (Thermo-Orion[®] Portable Meter Kit, STARA3295). Plate-type sediment DGTs and DETs
166 were deployed in shallow areas (water with a depth of less than 1.5 m) and in places with a

167 soft sediment bottom without sea grass. The probes were vertically pushed from the water
168 to the sediment by snorkeling with utmost care to prevent rupture in the filter and diffusive
169 layers. Before deployment, the probes were de-oxygenated by $N_{2(g)}$ for at least 24 hours in
170 the laboratory, and the de-aeration was continued during field deployment by portable
171 nitrogen tanks. The probes were deployed in anoxic sediment within one minute of removal
172 from the de-aerated water.

173 After two to three days of on-site deployment, the DGTs and DETs were retrieved
174 with careful snorkeling. After retrieval, each probe was carefully rinsed with site waters and
175 stored on ice in a clean Ziploc[®] bag. Especially for the sediment DET, 1 M NaOH was
176 pipetted at the surface of the filter within one minute after retrieval to stabilize Mn^{2+} and Fe^{2+}
177 by oxidizing the elements.¹⁹ As part of the retrieval process, sediment cores were taken to
178 measure particulate organic carbon in a laboratory. More details about the coring and
179 analysis are discussed in supporting documentation.

180

181 **Post-deployment laboratory analyses**

182 The DGTs and DETs were transported to laboratories at Daegu University and GIST
183 in South Korea for post-deployment processing. The probes were carefully rinsed with DI
184 water; resin gels for THg, CH_3Hg^+ , PO_4^{3-} , and S^{2-} , and diffusive gels for Mn and Fe were
185 removed from the probes. Accumulated species were directly extracted from resin gels in
186 circular-type DGTs. Resin gels in plate-type sediment probes were sliced with 1 cm
187 resolution and soaked in an appropriate extractant. The various extraction and measurement
188 techniques are summarized in **Table 2**.

189 To extract CH_3Hg^+ , 3MFSG gels were soaked in 4 mL of acidic thiourea solution
190 (1.13 mM thiourea + 0.1 M HCl) for 24 hours.²² The extractant was diluted in 100 mL of

191 DI water and converted to gaseous CH_3Hg^+ by aqueous phase ethylation using a
192 tetraethylborate solution. The volatile CH_3Hg^+ was then purged and trapped onto Tenax[®]
193 traps, which were flash-heated in a nitrogen stream. The released Hg species were
194 thermally separated on a GC column, then detected by CVAFS (Model III, Brooks Rand
195 Labs).

196 To extract THg, 3MFSG gels were soaked in 4 mL of 20% BrCl solution for 24 hours.
197 The excess oxidant was neutralized by adding hydroxylamine hydrochloride solution prior to
198 analysis. Hg in these samples was reduced to elemental Hg by SnCl_2 solution, and the
199 elemental Hg was contained in gold traps. The Hg^0 released from the gold traps by thermal
200 desorption was fed into a CVFAS.

201 To extract PO_4^{3-} , ferrihydrite resin gels were soaked in 1.5 mL of 0.25M H_2SO_4 for
202 24 hours, and the molybdenum blue method was used to determine PO_4^{3-} colorimetrically.
203 Reagent was prepared by mixing 500 ml of 2.5 M H_2SO_4 , 50 ml potassium antimony tartrate
204 solution, 150 ml ammonium molybdate solution, and 300 ml ascorbic acid solution. Then,
205 0.4 mL of the mixture was added to 5.0 mL of the samples, and absorbance at 880 nm was
206 determined using UV spectrophotometer (MECASIS).

207 Densitometry was used to determine the S^{2-} levels accumulated in the $\text{AgI}_{(s)}$ gel with
208 a slight modification.³⁰ $\text{AgI}_{(s)}$ resin gels with an area of 1.33 cm^2 were prepared and
209 immersed in 12 mL amber vials filled with 10 mL of deaerated DI water. Then, the vials
210 were spiked using S^{2-} with a concentration range from 0.0 – 1.46 μmol by adding 0.0163 M
211 S^{2-} stock solution prepared from $\text{Na}_2\text{S}\cdot 9\text{H}_2\text{O}_{(s)}$ and standardized with iodometric titration.
212 After a 24 hour solution equilibration, the resin gels were removed and placed on the
213 transparent OHP film with the binding side face-up and fixed with transparent tape over the
214 gel to protect the surface. The OHP film was then placed in a flat-bed scanner (Samsung
215 SCX-472x), and the image was recorded with a resolution of 300 DPI and saved as a TIFF

216 file using Adobe Acrobat Pro 9[®]. The greyscale intensity (0 – 255) of the scanned image
217 was measured using Adobe Photoshop CS3[®]. The greyscale intensity of the resin gels was
218 recorded considering the background greyscale intensity of blank AgI_(s) resin gels. The
219 AgI_(s) resins deployed in the sediments were also placed on OHP film protected by
220 transparent tape and without slicing. They were scanned, and greyscale intensity was
221 recorded. Using the standard curve evaluated above, the mass accumulated in resin was
222 calculated. More information about S²⁻ densitometry is available in the supporting
223 information.

224 To extract Fe and Mn from the diffusive gel of the DET probe, the gels were soaked
225 in 5 mL of 1 M HNO₃ for 24 hours, and the Fe and Mn were measured using ICP-OES
226 (Optima 7300DV).

227

228 **DGT data interpretation**

229 The concentrations of species in the water column and sediment pore water were
230 calculated by the following equation¹⁸:

$$231 \quad C_b = \frac{M \times \Delta g}{D \times t \times A} \quad (1)$$

232 where C_b is the labile metal species concentration in water [M L⁻³]; M is the mass of the
233 species accumulated in resin [M]; t is the deployment time [T]; D is the diffusion coefficient
234 of the species in the hydrogel [L² T⁻¹]; A is the exposed interfacial area [L²]; and Δg is the
235 total thickness of the diffusion layer [L], including the filter membrane and diffusive gel.
236 The diffusion coefficient of ions and metals depends on the temperature and can be corrected
237 using following equation:

$$\text{Log } D = \frac{\{1.37 \times (T - 25) + 8.36 \times 10^{-4} \times (T - 25)^2\}}{(109 + T)} + \text{Log} \left(D_{25} \times \frac{(273 + T)}{298} \right) \quad (2)$$

where D and D_{25} are the diffusivity of ions [$\text{L}^2 \text{T}^{-1}$] at $T^\circ\text{C}$ and 25°C , respectively.

240

241 Results

242 Overlying water quality

243 In the five locations, the average (\pm standard deviation) values of pH, dissolved
244 oxygen, and temperature ($n=16$) were relatively stable during probe deployment and retrieval.
245 These values were $6.79 (\pm 0.3)$, $5.25 (\pm 0.33) \text{ mg L}^{-1}$, and $28.2^\circ\text{C} (\pm 0.3)$, respectively.
246 Detailed values are available in **Table 3**. The conductivity was also stable at $85.4 (\pm 5.8) \mu\text{S}$
247 cm^{-1} from locations 1 to 4, confirming the waters were fresh, although the conductivities at
248 location 5 were varied between $5,500 \mu\text{S cm}^{-1}$ (~ 2.5 psu) and $10,310 \mu\text{S cm}^{-1}$ (~ 5.2 psu).
249 These measurements suggest that only location 5 (Cua Tieu estuary) was strongly influenced
250 by seawater intrusion from the adjacent South China Sea.

251 The DGT-measured THg and CH_3Hg^+ in overlying water (September 2013) were
252 comparable to the values in the previous grab sampling event during the dry season (April
253 2011) at the river.²⁷ The reported THg and CH_3Hg^+ in filtered overlying water (0.45 μm
254 polyethersulfone) varied from 1.2 to 14 pM and from 0.020 to 0.17 pM, respectively. DGT-
255 measured THg and CH_3Hg^+ varied from 1.16 to 34.5 pM and from 0.0026 to 0.072 pM,
256 respectively. The THg measured by DGT was similar to the grab sampling data, although
257 the DGT-measured CH_3Hg^+ concentrations were approximately two times lower than those
258 measured in the grab sampling. Care should be taken when making the comparison since
259 samplings were conducted during different (wet versus dry) seasons, and the seasonal effect
260 may lead to differences in CH_3Hg^+ concentrations. In addition, during the dry season in

261 2011, algal bloom was observed in the area, which led to lower dissolved CH_3Hg^+
262 concentrations in the water.²⁷ The discrepancy between the CH_3Hg^+ concentrations could
263 be associated with the inter-annual variations in CH_3Hg^+ production in the area.

264 In the present study, there were no significant and clear horizontal and vertical
265 distribution trends of THg and CH_3Hg^+ observed in the overlying water. The horizontal
266 trends were determined by comparing measurements from each location, and the vertical
267 distributions were determined by comparing measurements at different water depths.
268 Sediment is often considered the source of metals and nutrients, so higher levels of the
269 species in deeper water columns are expected from sediment fluxes. Probably due to the
270 small sample size, it was difficult to observe this trend. More extensive deployment of DGT
271 is necessary to understand seasonal variations and horizontal and vertical distributions of the
272 species in the water column of the Tien River.

273

274 **Porewater concentrations**

275 The DGT-measured vertical profiles of PO_4^{3-} , Mn, Fe, S^{2-} , THg, and CH_3Hg^+ in fresh
276 water and brackish water are shown in **Fig. 3 (a) – (f)**. The concentrations of THg and
277 CH_3Hg^+ in pore water were 1 – 2 orders of magnitude higher than in the overlying water (**Fig.**
278 **2**), thus, diffusive fluxes of the species from the sediment to overlying water were expected.
279 The concentrations of the measured species gradually escalated with the increased sediment
280 depth, although the vertical depths showing maximum concentrations were different
281 depending on the species. One location was selected in each environment (fresh and
282 brackish waters), therefore the comparisons between the locations were carefully made.
283 Additional studies using replicated sampling locations would provide more valuable
284 information include greater confidence in the comparisons.

285 In **Fig. 3 (a)**, the PO_4^{3-} concentrations were increased from 0.12 to 0.77 μM in

286 fresh and increased from 0.18 to 1.52 μM in brackish sediment. The PO_4^{3-} levels in
287 brackish sediment were two times higher than in fresh sediment. Similar vertical profiles
288 were observed for S^{2-} and are shown in **Fig. 3 (d)**. The S^{2-} concentrations were low (0 – 0.3
289 μM) at the surficial sediments from oxidation by O_2 , which was expected. However, the
290 levels increased to the maximum concentrations of 2.6 and 4.1 μM in fresh and brackish
291 sediments, respectively. The S^{2-} levels in brackish sediment were also two times higher than
292 in fresh sediment. This observation was consistent with a previous study that showed higher
293 SO_4^{2-} concentrations in brackish water (946 – 2862 mg L^{-1}) compared to fresh water (~ 14 mg
294 L^{-1}) and higher acid volatile sulfides in brackish water sediment (3.6 ± 2.6 $\mu\text{mol g}^{-1}$) compared
295 to fresh water sediment (1.6 ± 1.7 $\mu\text{mol g}^{-1}$).²⁷

296 The Mn and Fe in **Fig. 3 (b)** and **(c)**, also showed low concentrations at the
297 surficial sediments. The concentrations of Mn and Fe were less than 0.4 mM at the surficial
298 sediments (1 cm) and increased to 0.4 and 7.3 mM in fresh and 0.3 and 3.6 mM in brackish
299 sediment. The increase of Mn and Fe in the pore waters was considered a result of the
300 reduction of iron and manganese oxides to Mn^{2+} and Fe^{2+} respectively.³¹ The Fe
301 concentrations were at least an order of magnitude greater than the Mn concentrations. In
302 fresh sediment, the Mn and Fe concentrations were greater than those in brackish sediment,
303 which probably suggests that iron and manganese reduction are more dominant
304 biogeochemical processes in fresh water sediment.³²

305 The vertical profiles of THg and CH_3Hg^+ in **Fig. 3 (e)** and **(f)**, were similar, however,
306 they were different from other species. Generally, the higher THg and CH_3Hg^+
307 concentrations were observed in near-surficial sediments (depth < 6 cm), and lower
308 concentrations were observed in deeper sediments (depth > 6 cm). These characteristic
309 profiles were also observed in previous studies conducted in riverine, estuarine, and marine
310 sediments.^{13,14} As shown in **Table S1** and **Fig. S2**, pore water THg concentrations in fresh

311 sediment (23.7 ± 13.0) were lower than those in brackish sediment (47.9 ± 13.7) pM, although
312 pore water CH_3Hg^+ concentrations were similar (1.18 ± 0.61 pM in fresh and 1.24 ± 0.67 pM
313 in brackish).

314

315 **Comparison with other environments**

316 The levels of the measured species were compared with reported values in other
317 areas to assess the level of contamination in the Mekong Delta. Reported PO_4^{3-}
318 concentrations were widely distributed, ranging from 1 to 150 μM in lakes, bays, and
319 intertidal sea grass beds in other areas.^{17,23,24,33} Reported S^{2-} concentrations generally varied
320 between 1 and 20 μM in estuarine sediment, and levels as high as 60 μM were also
321 observed.^{24,30} Reported Fe and Mn concentrations varied between 0.1 and 0.9 mM and
322 between 0.01 and 0.03 mM; the values in the Mekong were in a similar range as other
323 studies.^{12,17} The PO_4^{3-} and S^{2-} levels in the Mekong were in the lower range of the observed
324 levels, and Fe and Mn levels were close to the reported values. The reported CH_3Hg^+
325 concentrations ranged from 4.63 to 13.9 pM in a salt marsh, 4.63 to 9.26 pM in the bay, and
326 9.26 to 37.0 pM in a river located in the San Francisco Bay area.¹³ The pore water CH_3Hg^+
327 concentrations in the Mekong Delta sediment were generally lower than the observed values,
328 suggesting the area is less impacted by Hg. These comparisons suggest that the Mekong
329 Delta sediment is not particularly contaminated and more research, including the
330 investigation of multiple locations, is necessary.

331

332 **Discussion**

333 **Redox zonation and nutrient release in sediment**

334 To better understand the redox zonation, the vertical profiles of the species were

335 normalized by the maximum pore water concentrations of the individual species and re-
336 plotted in **Fig. 4 (a) – (f)**.

337 In the fresh water sediment, PO_4^{3-} and S^{2-} were first observed at 1 cm directly below
338 the sediment-water interface, and the concentrations gradually increased with depth. The
339 maximum concentrations of the species appeared at approximately 4 – 6 cm and extended to
340 about 10 – 12 cm. Similar profiles were observed for Mn and Fe. The Mn and Fe
341 appeared at depths of 1 and 3 cm respectively, which were slightly deeper than those of PO_4^{3-}
342 and S^{2-} . The concentrations of the species continuously increased, and the maximum
343 concentrations of Mn and Fe were observed in deeper sediment at approximately 9 and 15 cm
344 respectively. The profile of Fe was about 2 cm shifted toward deeper sediment compared to
345 Mn, suggesting that Mn^{4+} was reduced before Fe^{3+} .

346 In brackish water sediment, the vertical profiles of PO_4^{3-} , S^{2-} , Mn, and Fe were
347 different from fresh water sediment. The profiles of PO_4^{3-} and S^{2-} showed more rapid
348 increase in the pore water, producing sharper vertical gradients at the surficial sediment.
349 The maximum concentrations of PO_4^{3-} and S^{2-} were observed at sediment depths of
350 approximately 4 and 3 cm respectively. The maximum S^{2-} was detected between 2 and 3 cm
351 directly below the surface sediment. Note that the maximum S^{2-} was shown at a depth of
352 about 5 cm in fresh water sediment. The Mn and Fe concentrations also rapidly increased
353 from the interface, and maximum concentrations were detected at an approximate depth of 6
354 cm; the concentrations then began to decrease. The depths for maximum Mn^{2+} and Fe^{2+} in
355 the brackish sediment were closer to the sediment-water interface compared to those in the
356 fresh water sediment.

357 The particulate organic matter measured by loss on ignition (550°C) at surficial 8 cm
358 sediments were higher in brackish water sediment ($7.81\pm 0.44\%$) compared to fresh water
359 sediment ($5.85\pm 1.3\%$) (**Table S3**). The higher organic matter concentrations (i.e., energy

360 for microorganism metabolism and higher SO_4^{2-} in brackish water probably increased the
361 activities of anaerobic microorganisms and induced more intensive biogeochemical reactions
362 in surficial sediments.

363 It is generally assumed that electron acceptors (EA), such as O_2 , NO_3^- , $\text{MnO}_{2(s)}$,
364 $\text{Fe}(\text{OH})_{3(s)}$, and SO_4^{2-} , are sequentially reduced in order from the most energy-yielding to the
365 lowest energy-yielding EA when microorganisms decompose organic matter as an electron
366 donor.³⁴ However, in the fresh and brackish water sediments, the vertical profiles of Fe and
367 S^{2-} (shown in **Fig. 4**) suggested that SO_4^{2-} seemed to be reduced before Fe^{3+} , or the two
368 electron acceptors were reduced simultaneously. Theoretical calculations in realistic
369 environmental conditions, and several field observations suggest that simultaneous reduction
370 of Fe^{3+} and SO_4^{2-} is thermodynamically possible under a wide range of sedimentary
371 environmental conditions and that SO_4^{2-} reduction may occur before Fe^{3+} reduction.^{7,24}

372 In addition, the release of PO_4^{3-} seems tightly coupled with the release of S^{2-} in the
373 two sediments (see **Fig. 5**). The PO_4^{3-} is believed to be strongly adsorbed in iron oxide and,
374 when reduced, Fe^{2+} and PO_4^{3-} tend to release simultaneously.³⁵ However, the simultaneous
375 release of PO_4^{3-} and S^{2-} has also been observed.²⁴ A previous study showed that the Fe^{2+}
376 and PO_4^{3-} concentrations in sea grass-sediment pore water did not coincide when the two
377 species were compared in a two-dimensional graph, although they seemed well related in a
378 one-dimensional graph.¹⁷ In marine environments, S^{2-} appears to induce phosphate release
379 from marine microorganisms.³⁶ In addition, evidence shows that PO_4^{3-} release may
380 originate from benthic microorganisms via polyphosphate metabolism, rather than iron
381 reduction and adsorbed- PO_4^{3-} release.³⁷ More research is necessary to understand the
382 coupled biogeochemical reactions that release PO_4^{3-} , Fe^{2+} , and S^{2-} in sediment pore water.

383

384 **Mercury methylation in sediments**

385 As shown in **Fig. 4 (c) and (f)**, the profiles of THg and CH_3Hg^+ were similar,
386 however, they were distinct compared to other species in sediment pore water. In fresh
387 water sediment, the concentrations of THg and CH_3Hg^+ increased with sediment depth, and
388 maximum concentrations were observed at a depth of approximately 3 – 4 cm. The
389 concentrations then decreased with the increase of sediment depth. In contrast, two distinct
390 peaks of maximum THg and CH_3Hg^+ concentrations were observed in brackish water
391 sediment pore water. The first peak materialized directly below the water-sediment
392 interface at a depth of approximately 0 – 1 cm, and the second peak was observed at a depth
393 of roughly 6 – 7 cm. The first CH_3Hg^+ maximum in fresh and brackish water sediments was
394 detected directly above the area where the S^{2-} maximum concentrations began to build up.
395 The second CH_3Hg^+ maximum in brackish water sediment corresponds to the area where the
396 Mn and Fe maximum concentrations were observed.

397 Several processes for microbial uptake of Hg^{2+} procures CH_3Hg^+ in an aquatic
398 environment.¹ A passive diffusion mechanism of uncharged, dissolved Hg complexes such
399 as HgS^0 is probably the most widely studied process.^{38,39} The mechanism is strongly
400 dependent on the level of dissolved HgS^0 in anoxic water, which is highly dependent on S^{2-}
401 concentrations. The HgS^0 concentrations are dominant species at S^{2-} concentrations greater
402 than 10^{-9} M. However, at S^{2-} concentrations greater than 10^{-5} M, the HgS^0 species shift to
403 charged, non-bioavailable complexes, such as HgS_2^{2-} and HgS_2H^- .^{39,40} Hence, the decrease
404 of bioavailable Hg^{2+} species (and, therefore, low CH_3Hg^+ concentrations) in the presence of a
405 high S^{2-} environment ($>10^{-5} - 10^{-4}$ M) has been observed in estuarine and marine
406 environments.^{41,42}

407 This study's observations of the first CH_3Hg^+ maximum near surficial sediments
408 immediately before S^{2-} maximum probably support the previous observations and suggest
409 that the CH_3Hg^+ production in the Mekong Delta sediment is coupled with SO_4^{2-} reduction.

410 It is well established that DGT can underestimate pore water concentrations of a species
411 when resupply kinetics of a species from solid are slow and when the species pool is small.⁴³
412 Considering the use of DGT may deplete pore water S^{2-} concentrations, and the acid volatile
413 sulfides were relatively low in the two sediments, the actual pore water S^{2-} concentrations
414 could be higher than the calculated values. It is possible that the elevated S^{2-} concentrations
415 in sediment pore water reduced the bioavailable HgS^0 in deeper sediments, which decreased
416 Hg^{2+} methylation in the pore water. The alternative is that the sediment layer between the
417 sulfide and Fe maximum (4 – 14 cm for fresh sediment and 3 – 7 cm for brackish sediment)
418 could be enriched with solid FeS (i.e., AVS) that limits the microbial Hg^{2+} methylation.⁴⁴

419 The second CH_3Hg^+ peak in brackish water sediment seems to be more related to
420 iron reduction processes. Iron and manganese oxides appear to reduce significantly at a
421 depth of approximately 6 cm, and Hg seems to be methylated simultaneously during the
422 reduction reactions. In some studies, iron-reducing bacteria can produce CH_3Hg^+ ,⁶ and the
423 production and mobility is tied to the Fe redox cycling in the sediment.¹⁴

424

425 **Flux calculations**

426 Estimating the diffusive flux of THg and CH_3Hg^+ from sediment overlying water is
427 important for assessing the sediment contamination and managing Hg risks in a body of water.
428 The diffusive flux at the sediment water interface was calculated using the following
429 equation:

$$430 \quad \text{Flux} = -\frac{\theta D_w}{1 - \ln(\theta^2)} \frac{dC}{dx} \quad (3)$$

431 where D_w is the diffusivity of THg or CH_3Hg^+ [$L^2 T^{-1}$]; θ is the porosity of sediments
432 [unitless]; dC is the THg or CH_3Hg^+ concentration difference between water column (C_w) and
433 sediment pore water (C_{pw}) [$M L^{-3}$]; and dx is the average sediment depth used to measure C_{pw}

434 [L]. **Table 4** summarizes the flux calculations. The first 1-cm depth-averaged pore water
435 THg and CH₃Hg⁺ concentrations were used for C_{pw}, and the depth-averaged overlying water
436 THg and CH₃Hg⁺ concentrations shown in **Fig 2 (b)** and **(c)** were used for C_w. In fresh and
437 brackish sediments, the calculated THg fluxes to overlying water were 4.3 and 23.6 ng m⁻² d⁻¹
438 respectively, and the CH₃Hg⁺ fluxes were 0.33 and 2.92 ng m⁻² d⁻¹ respectively. The
439 CH₃Hg⁺ fluxes were about 8 – 12% of the THg fluxes to overlying water. Although the
440 surface 10-cm averaged THg concentrations in brackish sediment were only two times
441 greater than in the fresh sediment (**Table S2**), the calculated THg diffusive fluxes were five
442 times greater in the brackish sediment. This observation was even more drastic for CH₃Hg⁺.
443 The CH₃Hg⁺ concentrations in the two sediment pore waters were similar (in **Table S2**);
444 nonetheless, the flux to overlying water was eight times higher in brackish than in fresh water
445 sediment. The grab sampling of the surficial sediments may not have captured the sharp
446 concentration gradients of CH₃Hg⁺ in sediment pore water, and may have calculated biased
447 diffusive fluxes. Measuring pore water CH₃Hg⁺ concentrations with high resolution is
448 considered important for estimating diffusive fluxes of the species in sediment.

449 Diffusive fluxes of THg (ng m⁻² d⁻¹) were reported as 1.7 – 30 in a bay⁹ and 710 –
450 1590 in an estuary.^{45,46} Diffusive fluxes of CH₃Hg⁺ (ng m⁻² d⁻¹) were reported as 0.16 in a
451 lake; 10.1 in a river; 0.03 – 27.4 in a Delta; and 15.1 – 42 in a bay.¹³ Direct comparisons of
452 the estimated fluxes might not be possible since the fluxes could be highly heterogeneous
453 depending on the biogeochemical conditions of the sites. Nevertheless, the estimated fluxes
454 of THg and CH₃Hg⁺ in the Mekong Delta were in the lower range of the reported values,
455 which further suggests that the area has relatively low risk.

456

457 **Conclusions**

458 DGT and DET techniques were applied to the Tien River in Vietnam's Mekong Delta
459 to assess Hg contamination and to understand how redox zonation affects Hg methylation.
460 Elevated S^{2-} concentrations were detected in the shallower depth in brackish compared to
461 fresh sediments, suggesting that copious SO_4^{2-} was reduced in near surficial sediments in
462 brackish sediments. This redox status seemed to drive pore water CH_3Hg^+ maximum in the
463 shallower depth with higher concentrations, which resulted in a CH_3Hg^+ flux approximately
464 eight times higher in the brackish than fresh sediments. Accurate measurement of pore
465 water CH_3Hg^+ concentrations without disturbance would be critical for estimating such
466 diffusive fluxes of the species in aquatic environments. The release of PO_4^{3-} seems to be
467 related with S^{2-} release, suggesting PO_4^{3-} release may be more related to sulfate reduction
468 than iron reduction, a process commonly correlated with PO_4^{3-} release.

469 For better quantitative use of DGT, future research should be directed to accurately
470 estimate dissolved chemical species in pore water.⁴³ The application of DETs for redox
471 sensitive species such as PO_4^{3-} and S^{2-} could be an appropriate approach, as it minimizes the
472 decrease of the species during pore water collection and processing. For THg and CH_3Hg^+ ,
473 deployment of multiple DGT probes with different diffusive thicknesses¹² would be effective
474 in estimating actual porewater concentrations when DGTs are deployed in environments
475 where the resupply kinetics of the species are slow.¹² In addition, fine resolution (~ mm)
476 measurements of Hg in sediment pore water could provide notable information on the Hg
477 biogeochemical reactions that have not been observed and reported. Lastly, further studies
478 are necessary in the Mekong Delta to understand which biogeochemical conditions (e.g.,
479 sediment organic matter) mainly control Hg methylation, and samplings in replicated
480 locations are necessary to obtain site representative information.

481

482 **Acknowledgement**

483 The authors thank Bo-Kyung Kim from GIST and Se-Hee Lee from Daegu University for
484 their support in collecting samples. This work was supported by the National Research
485 Foundation of Korea Grant funded by the Korean Government (NRF-
486 2012R1A2A2A06046793) and the Ministry of Science, ICT and Future Planning through the
487 UNU & GIST Joint Program.

488

489

490 **Table 1** Summary of DGT and DET used in the present study. For all circular type overlying probes and plate type sediment probes, polysulfone
491 and Millipore Durapore PVDF (hydrophilic polyvinylidene fluoride) with 0.45 μm pore size were used, respectively.

Target Species	Probe Type	Resin Gel Composition	Diffusive Gel	Extractant	Extraction Efficiency	Reference
CH_3Hg^+	DGT	2 g of 3MPFS in 10 mL of GS1	GS3 ^c	1.13 mM Thiourea + 0.1M HCl	0.91	22, 29
THg	DGT	2 g of 3MPFS in 10 mL GS1	GS3	20% BrCl ^b	1.0	29, 47
PO_4^{3-}	DGT	6 g of FPF in 10 mL GS2	GS3	0.25 M H_2SO_4	0.98 ^c	23
S^{2-}	DGT	1 g of $\text{AgI}_{(s)}$ in GS1	GS1	NA	-	30
Fe, Mn	DET	NA	GS1	1.0 M HNO_3	-	19

492 a. Summary of acronyms: 3MPFS=3-mercaptopropyl functionalized silica gel (Sigma Aldrich); FPF=freshly precipitated ferrihydrite slurry;
493 GS1=gel solution 1 (15 mL agarose solution from DGT research + 37.5 mL 40% acrylamide solution + 47.5 mL H_2O); GS2=gel solution
494 2 (100 mL solution containing 28.5 g acrylamide + 1.5 g bisacrylamide); GS3=gel solution 3 (1.5 g arose gel in 10 mL DI water)

495 b. 27 g KBr+ 38 g KBrO_3 in 2.5 L concentrated HCl

496 c. Re-evaluated in the present study

497

498 **Table 2** Summary of diffusion coefficients used to convert DGT accumulated mass to
499 pore water concentration.

Species	D ($10^{-6} \text{ cm}^2 \text{ s}^{-1}$)		Reference
	25°C	29°C	
THg ^a	4.0	4.41	29
CH ₃ Hg ⁺	5.26	5.80	
PO ₄ ³⁻	6.05	6.67	23
S ²⁻	14.8 ^b	16.3	30

500 a. Assumed mostly consist of Hg²⁺

501 b. A value at 18°C

502

503

504

505

506

507

508

509

510

511

512

513

514

515

516 **Table 3.** Summary of location information and water quality measurements.

517

ID	latitude	longitude	water depth (m)	deployment time (days)	values during deployment – values during retrieval			
					pH	conductivity ($\mu\text{S cm}^{-1}$)	DO (mg L^{-1})	temperature ($^{\circ}\text{C}$)
L1	10.31916	106.02000	5.7	2.79	7.32 – 6.87	79.80 – 80.14	5.52 – 5.61	28.0 – 28.0
L1 ^a	10.32333	106.03000	-	2.85	7.10 – 7.23	84.40 – 79.75	5.80 – 4.94	28.1 – 28.5
L2	10.31583	106.20055	27.7	2.73	7.09 – 6.14	81.21 – 86.57	4.97 – 5.49	27.7 – 28.1
L3	10.34805	106.35055	8.4	2.18	6.97 – 6.91	87.78 – 84.01	5.01 – 5.24	27.8 – 28.0
L4	10.30750	106.50361	8.6	2.10	6.98 – 6.88	94.23 – 95.71	4.93 – 5.75	28.5 – 28.2
L5	10.26000	106.75527	6.5	2.03	7.01 – 7.36	9657 – 5500	5.32 – 4.91	28.0 – 28.0
L5 ^a	10.26888	106.75083	-	2.07	7.23 – 6.56	10310 – 3890	5.23 – 4.64	28.5 – 28.4

518 a. Locations that sediment pore water DGTs and DETs were deployed.

519

520

Table 4 Fluxes of CH_3Hg^+ from sediment to overlying water using the surface 1 cm averaged pore water CH_3Hg^+ concentrations determined by DGT and equation (3). In fresh and brackish water sediments, diffusion coefficients³ of THg and CH_3Hg^+ were 4.41×10^{-6} and $5.8 \times 10^{-6} \text{ cm}^2 \text{ s}^{-1}$ at 29°C , respectively, and porosities (θ) were 0.58 and 0.79, respectively. The dx was 0.5 cm.

Environment	-dC (=C _{pw} - C _w)		Flux	
	THg (ng L ⁻¹)	CH ₃ Hg ⁺ (pg L ⁻¹)	THg (ng m ⁻² d ⁻¹)	CH ₃ Hg ⁺ (ng m ⁻² d ⁻¹)
Fresh	2.1 (=3.7 - 1.6)	112 (=116 - 4)	4.3	0.33
Brackish	5.8 (=8.6 - 2.8)	455 (=464 - 9)	23.6	2.92

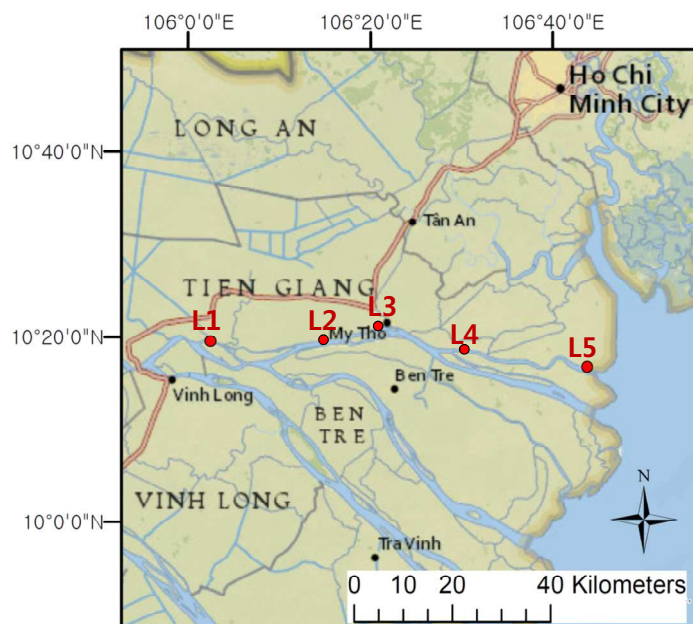


Fig. 1 Map of the Mekong River Delta showing the location of DGT and DET deployment locations. DGTs were deployed in the overlying waters of L1 – L5. DGTs and DETs were deployed in the sediments of L1 (fresh) and L5 (brackish).

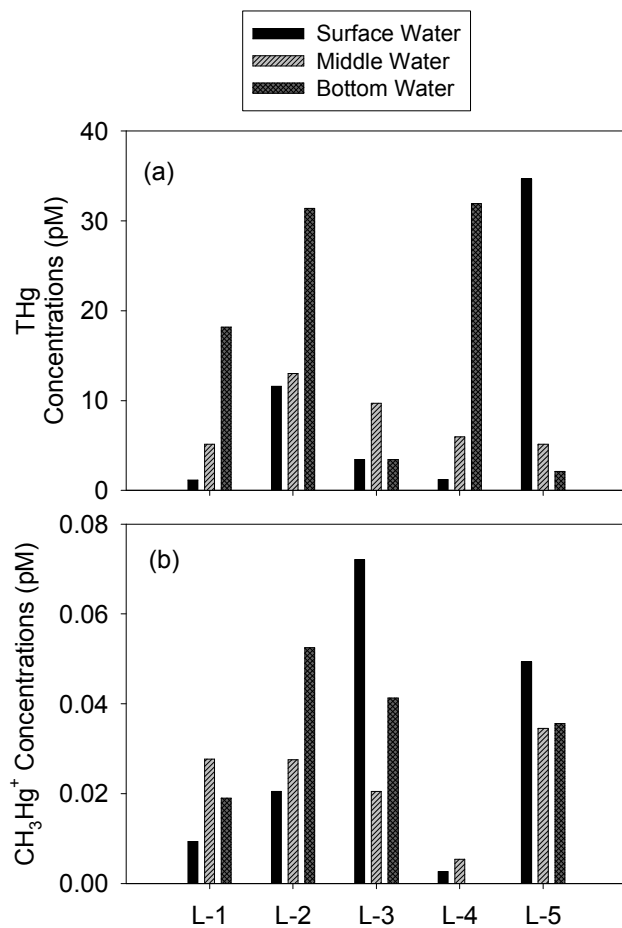


Fig. 2 The vertical and horizontal distribution of DGT measured (a) THg and (b) CH₃Hg⁺ concentrations in the water column of Tien River, Mekong Delta, Vietnam.

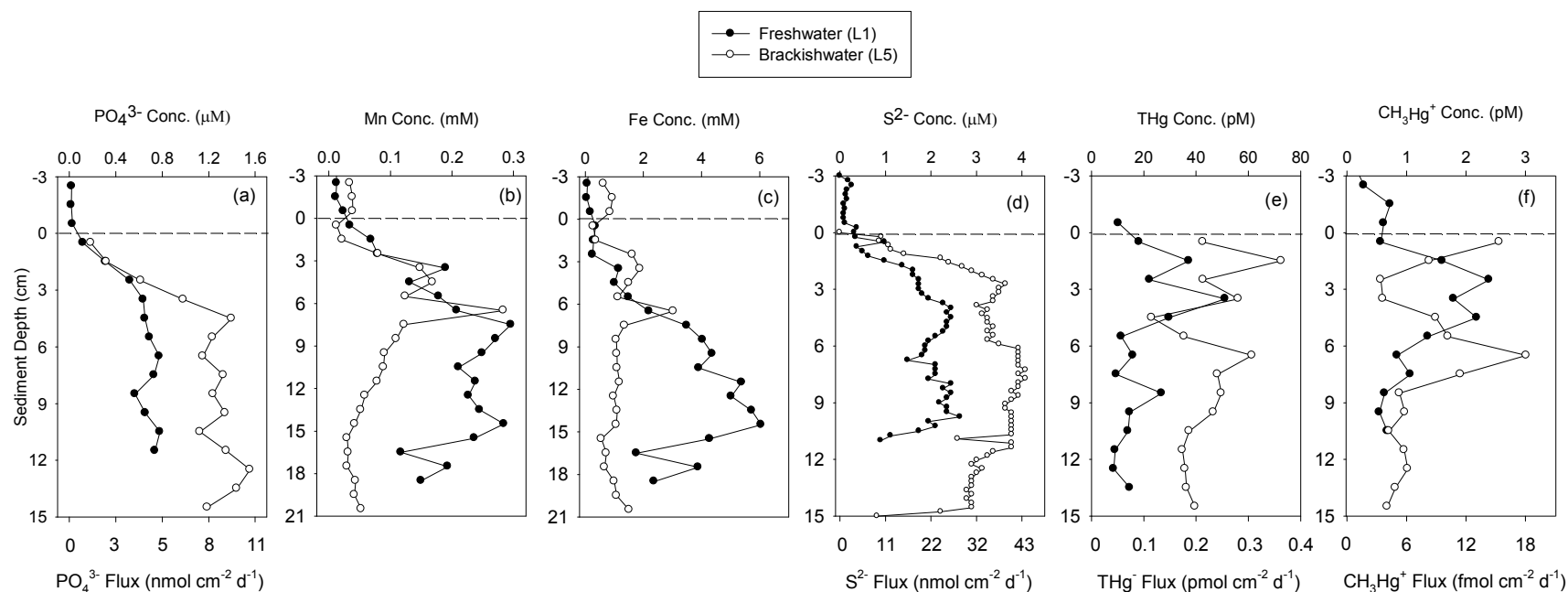


Fig. 3 The vertical pore water concentrations of DGT or DET measured (a) PO_4^{3-} , (b) Mn, (c) Fe, (d) S^{2-} , (e) THg, and (f) CH_3Hg^+ in fresh water (solid circles) and brackish water (hollow circles) sediments of the Tien River, Mekong Delta, Vietnam. Note that the DGT measurements were also shown as flux ($=M/At$, where M is the mass accumulated in resin, A is the exposed area, and t is the deployment time)

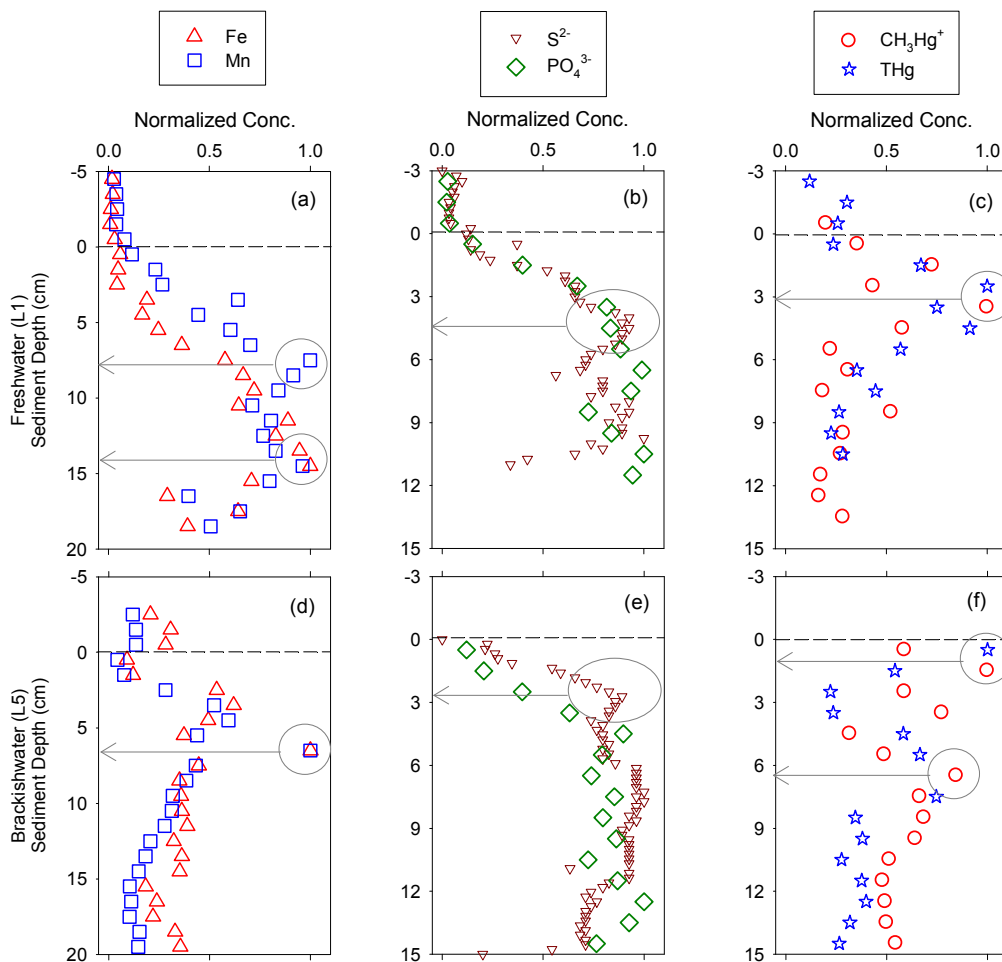


Fig. 4 The normalized vertical pore water levels of (a)/(d) Mn, Fe, (b)/(e) PO_4^{3-} , S^{2-} , and (c)/(f) THg, CH_3Hg^+ measured by DGT or DET in the Tien River, Mekong Delta, Vietnam. The arrows indicate the sediment depths correspond to maximum concentrations of the species.

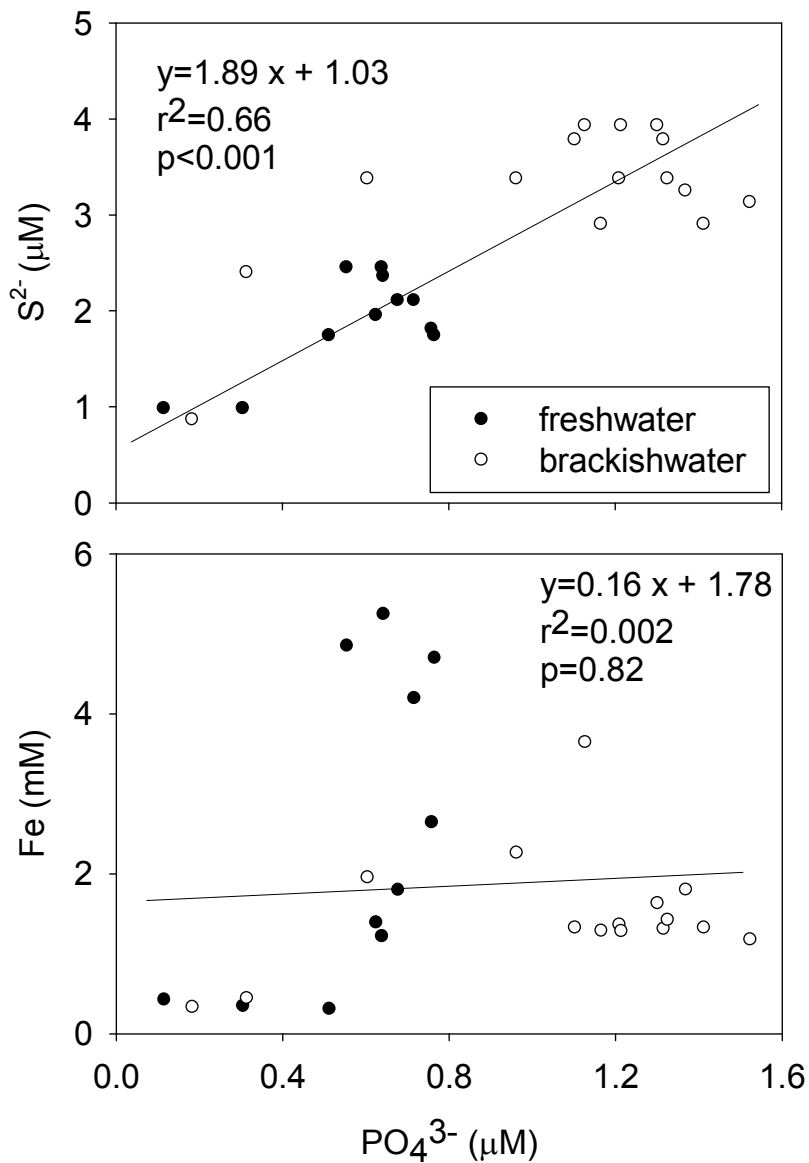


Fig. 5 The correlation between PO_4^{3-} and S^{2-}/Fe in sediment pore water of Tien River, Mekong Delta, Vietnam.

References

1. H. Hsu-Kim, K. H. Kucharzyk, T. Zhang and M. A. Deshusses, *Environmental Science & Technology*, 2013, 47, 2441-2456.
2. C. T. Driscoll, R. P. Mason, H. M. Chan, D. J. Jacob and N. Pirrone, *Environmental Science & Technology*, 2013, 47, 4967-4983.
3. C. C. Gilmour, M. Podar, A. L. Bullock, A. M. Graham, S. D. Brown, A. C. Somenahally, A. Johs, R. A. Hurt, K. L. Bailey and D. A. Elias, *Environmental Science & Technology*, 2013, 47, 11810-11820.
4. UNEP, *Global Mercury Assessment*, UNEP/Inter-Organization Programme for the Sound Management of Chemicals, Geneva, Switzerland, 2002.
5. C. C. Gilmour, E. A. Henry and R. Mitchell, *Environmental Science & Technology*, 1992, 26, 2281-2287.
6. E. J. Kerin, C. C. Gilmour, E. Roden, M. Suzuki, J. Coates and R. Mason, *Applied and environmental microbiology*, 2006, 72, 7919-7921.
7. D. Postma and R. Jakobsen, *Geochimica et Cosmochimica Acta*, 1996, 60, 3169-3175.
8. B. P. Boudreau, *Diagenetic models and their implementation : modelling transport and reactions in aquatic sediments*, Springer, Berlin ; New York, 1997.
9. G. A. Gill, N. S. Bloom, S. Cappellino, C. T. Driscoll, C. Dobbs, L. McShea, R. Mason and J. W. M. Rudd, *Environmental Science & Technology*, 1999, 33, 663-669.
10. C. R. Hammerschmidt, W. F. Fitzgerald, C. H. Lamborg, P. H. Balcom and P. T. Visscher, *Marine Chemistry*, 2004, 90, 31-52.
11. R. Mason, N. Bloom, S. Cappellino, G. Gill, J. Benoit and C. Dobbs, *Environmental Science & Technology*, 1998, 32, 4031-4040.
12. H. Zhang, W. Davison, S. Miller and W. Tych, *Geochimica et Cosmochimica Acta*, 1995, 59, 4181-4192.
13. O. Clarisse, B. Dimock, H. Hintelmann and E. P. H. Best, *Environmental Science & Technology*, 2011, 45, 1506-1512.
14. N. S. Bloom, G. A. Gill, S. Cappellino, C. Dobbs, L. McShea, C. Driscoll, R. Mason and J. Rudd, *Environmental Science & Technology*, 1998, 33, 7-13.
15. K. A. Merritt and A. Amirbahman, *Environ Sci Technol*, 2007, 41, 717-722.
16. N. A. Hines, P. L. Brezonik and D. R. Engstrom, *Environ Sci Technol*, 2004, 38, 6610-6617.
17. A. Pagès, P. R. Teasdale, D. Robertson, W. W. Bennett, J. Schäfer and D. T. Welsh, *Chemosphere*, 2011, 85, 1256-1261.

18. H. Zhang and W. Davison, *Anal Chem*, 1995, 67, 3391-3400.
19. W. Davison, H. Zhang and G. W. Grime, *Environmental Science & Technology*, 1994, 28, 1623-1632.
20. W. J. Li, J. J. Zhao, C. S. Li, S. Kiser and R. J. Cornett, *Analytica Chimica Acta*, 2006, 575, 274-280.
21. H. Docekalova and P. Divis, *Talanta*, 2005, 65, 1174-1178.
22. O. Clarisse and H. Hintelmann, *J Environ Monitor*, 2006, 8, 1242-1247.
23. H. Zhang, W. Davison, R. Gadi and T. Kobayashi, *Analytica Chimica Acta*, 1998, 370, 29-38.
24. S. Ding, Q. Sun, D. Xu, F. Jia, X. He and C. Zhang, *Environ Sci Technol*, 2012, 46, 8297-8304.
25. A. Snidvongs and S. Teng, *Global International Waters Assessment, Mekong River, GIWA Regional assessment 55*, University of Kalmar on behalf of United Nations Environment Programme, 2006.
26. MRC, *An assessment of water quality in the Lower Mekong Basin. MRC Technical Paper No.19. Mekong River Commission, Vientiane. 70 pp. ISSN: 1683-1489*, 2008.
27. S. Noh, M. Choi, E. Kim, N. P. Dan, B. X. Thanh, N. T. V. Ha, S. Sthiannopkao and S. Han, *Geochimica et Cosmochimica Acta*, 2013, 106, 379-390.
28. E. G. Pacyna, J. M. Pacyna, F. Steenhuisen and S. Wilson, *Atmospheric Environment*, 2006, 40, 4048-4063.
29. Y. S. Hong, E. Rifkin and E. J. Bouwer, *Environ Sci Technol*, 2011, 45, 6429-6436.
30. P. R. Teasdale, S. Hayward and W. Davison, *Anal Chem*, 1999, 71, 2186-2191.
31. Y. S. Hong, K. A. Kinney and D. D. Reible, *Environmental toxicology and chemistry / SETAC*, 2011, 30, 1775-1784.
32. D. Lovley and E. Phillips, *Appl Environ Microbiol*, 1987, 53, 2636-2641.
33. S. Ding, D. Xu, Q. Sun, H. Yin and C. Zhang, *Environ Sci Technol*, 2010, 44, 8169-8174.
34. R. Berner, 1980.
35. D. J, A. G, M. A, J. z. q. D, T. G, C. J, B. G and A. P, *Marine Ecology Progress Series*, 2008, 355, 59-71.
36. J. Brock and H. N. Schulz-Vogt, *ISME J*, 2011, 5, 497-506.
37. P. Sannigrahi and E. Ingall, *Geochemical Transactions*, 2005, 6, 52.
38. A. Drott, L. Lambertsson, E. Björn and U. Skyllberg, *Environmental Science & Technology*, 2007, 41, 2270-2276.

39. J. M. Benoit, C. C. Gilmour, R. P. Mason and A. Heyes, *Environmental Science & Technology*, 1999, 33, 951-957.
40. J. M. Benoit, R. P. Mason and C. C. Gilmour, *Environmental Toxicology and Chemistry*, 1999, 18, 2138-2141.
41. C. Gilmour, G. S. Riedel, M. C. Ederington, J. T. Bell, G. A. Gill and M. C. Stordal, *Biogeochemistry*, 1998, 40, 327-345.
42. J. M. Benoit and C. C. Gilmour, *ACS Symposium Series 835 (Biogeochemistry of Environmentally Important Trace Elements):262-297*, 2003.
43. M. P. Harper, W. Davison, H. Zhang and W. Tych, *Geochimica Et Cosmochimica Acta*, 1998, 62, 2757-2770.
44. C. R. Hammerschmidt and W. F. Fitzgerald, *Environ Sci Technol*, 2004, 38, 1487-1495.
45. N. Mikac, S. Niessen, B. Ouddane and M. Wartel, *Applied Organometallic Chemistry*, 1999, 13, 715-725.
46. M. Coquery, D. Cossa and J. Sanjuan, *Marine Chemistry*, 1997, 58, 213-227.
47. A. Amirbahman, D. I. Massey, G. Lotufo, N. Steenhaut, L. E. Brown, J. M. Biedenbach and V. S. Magar, *Environmental science. Processes & impacts*, 2013, 15, 2104-2114.